Neonatal CD4+ T cells have a characteristic transcriptome and epigenome and respond to TCR stimulation with proliferation and yet a limited immune response

Linda Aimara Kempis-Calanis, Otoniel Rodríguez-Jorge, Darely Yarazeth Gutiérrez-Reyna, Carlos Jesús Ventura-Martínez, Salvatore Spicuglia, Alejandra Medina-Rivera, Denis Thieffry, Aitor González, María Angélica Santana

Neonatal CD4+T cells have a characteristic transcriptome and epigenome and respond to TCR stimulation with proliferation and yet a limited immune response.

Kempis-Calanis L.A.[1#], Rodríguez-Jorge O.[1*#], Gutiérrez-Reyna D.Y.[1], Ventura-Martínez, C.J.[1], Spicuglia S.[4], Medina-Rivera, A.[2], Thieffry, D[3]., González, A.[4], , Santana M.A.[1*]

[1]Laboratorio de Inmunología Celular, Centro de Investigación en Dinámica Celular, Instituto de Investigación en Ciencias Básicas y Aplicadas, Universidad Autónoma del Estado de Morelos, 62210, Cuernavaca, México.
[2]Laboratorio Internacional de Investigación sobre el Genoma Humano, Universidad Nacional Autónoma de México, Juriquilla, México.
[3]Computational System Biology Team, Institut de Biologie de l'Ecole Normale Supérieure, CNRS UMR8197, INSERM U1024, PSL University.
[4]Aix-Marseille University, Inserm, TAGC, UMR1090, 13288, Marseille, France.

[#]These authors equally contributed to this work.
*These authors share the last authorship

Correspondence:
santana@uaem.mx
orj@uaem.mx

Keywords: Neonatal CD4$^+$ T cells, T_{REG}, Transcriptomics, epigenetic, enhancers.

Abstract

The adaptive immune response is coordinated by $CD4^+$ T cells, which determine the response type and strength and the effector cells involved during a particular immune challenge. It has been reported that $CD4^+$ T cells are less responsive in neonates, leading to poor antibody production and low activation of the cellular response. This low response is essential for the tolerant window that favors birth transition from the sterile environment in the womb to the outside world but leaves neonates vulnerable to infection, which is still an important health issue. Neonates have a morbidity and mortality rate due to infections, and the molecular reasons are still understudied.

Therefore, we asked whether the neonatal, compared to adult naive $CD4^+$ T cells, have a particular genomic structure that predisposes them to a regulatory network favoring a tolerant response. To answer this question, we evaluated the transcriptome and epigenome of human neonatal and adult naive $CD4^+$ T cells. Our results point to a very distinct regulatory network in neonatal cells, which favors a tolerant response through pathways related to regulatory cells, glucose metabolism, and cell function.

Understanding this network should lead to novel vaccine formulations and better deal with life-threatening diseases during this highly vulnerable period of our lives.

Introduction

Comprising the first 28 days of life, the neonatal period is the most vulnerable period for a child's health and survival. The number of deaths has declined over recent years, but on average 17 deaths per 1000 live births still occur worldwide. Infections account for around 24% of neonatal deaths and they are usually more severe and longer lasting (1). Infections mediated by intracellular pathogens are particularly dangerous in neonates, suggesting that T-cell-mediated immunity is limited in the early stages of life. Neonates have limited exposure to antigens in the mother's uterus, and so the naivety of its lymphocytes has been made responsible for its low response, particularly to intracellular pathogens (2) (3). Recent evidence suggests, however, that rather than being unable to respond, they do not respond as expected, because neonatal T cells have their own characteristics, adapted to the particular needs of the neonatal period (4, 5). A poor antibody response is also observed, perhaps due to a limiting expansion of T_{FH} cells and also a high expression of miR-181b (6-11).

It has been shown that neonatal $CD4^+$ T cells respond differently from adult cells, with a high production of IL-8 (12), a prevalent Th2 over Th1 profile, and an innate inflammatory response (3, 4). The IL-13 locus is open in neonatal cells and remains open upon differentiation into Th1 populations, confirming an epigenetic bias of neonatal cells towards the Th2 phenotype (13). At the level of cell signaling, neonatal $CD4^+$ T cells display enhanced calcium signals, probably mediated by miR181a, but reduced AP-1 activation, probably contributing to the lower activation of the cells (14). A recent study evaluating open chromatin regions of neonatal and adult $CD4^+$ T cells showed that the chromatin of adult cells is more open as compared to that of neonatal cells (15).

Metabolism plays an important role in the different stages of T cell activation and differentiation. Naive and memory T cells depend on the full oxidation of pyruvate through the Tricarboxylic acid cycle to generate reduction power (NADH and FADH2) and, after oxidative phosphorylation (OXPHOS), 36 molecules of ATP per molecule of glucose. After T cell activation, there is an increase in aerobic glycolysis, known as the Warburg effect, characterized by the conversion of pyruvate to lactate, to provide carbon skeletons for molecule biosynthesis, needed for cell proliferation and other demands of effector cells.

In our previous studies on neonatal $CD8^+$ T cells, we found a unique transcriptomic profile, biased towards innate immunity and homeostatic proliferation, with a low expression of cytotoxicity and signal transduction genes (16). Further, we found that these cells had an increased expression of glycolysis genes and a high production of Reactive Oxygen Species, which could lead to a lower activation (17). Based on a qualitative dynamical model of the corresponding network, we predicted that this could impact negatively cell activation (17). . Activation of neonatal $CD8^+$ T cells, however, was possible under strong activation conditions in the presence of IL-12, which induced a more balanced cell metabolism, among other changes (18).

In this study, we evaluated the transcriptomic profile of neonatal and adult naive $CD4^+$ T cells and showed that the neonatal cells have a characteristic transcriptome, in which pathways related to regulatory functions, aerobic glycolysis, proliferation, innate inflammation, cell motility, and cell signaling control were enriched, explaining the high threshold of cell activation. A specific set of hyperproliferative-related transcription factors,

such as *BCL11A* and *HOX* genes, were found overexpressed in the neonatal cells, at both the transcriptome and protein levels. Indeed, the neonatal cells proliferated more, under basal conditions as well as after activation.

Taking advantage of the BLUEPRINT data (19), we compared our the overexpressed genes in our transcriptome with that of the blue print data, finding equivalent overexpressed genes. We further analyzed the corresponding profiles of histone modification marks in neonatal and adult naive $CD4^+$ T cells and the combination of these marks. Using ChromHMM, we combined these marks to characterize the specific epigenetic landscape of neonatal $CD4^+$ T cells. Our analysis points to striking changes in promoters and enhancers between neonatal and adult cells, with stronger changes in the enhancer regions. Focusing on the most representative chromatin marks, the most significant difference between adult and neonatal $CD4^+$ T cells involved the closed chromatin mark H3K27me3, which was slightly higher in the neonatal-overexpressed regions in adult cells' filesand much higher in the adult overexpressed regions in neonatal cells' files. This suggests that the histone mark H3K27me3 maintains closed the adult-specific-genes in neonatal $CD4^+$ T cells. We also found differences in the functional analysis of genes near these active regulatory signals, with the strongest differences found in active enhancers. Neonatal $CD4^+$ T cell active regulatory regions are enriched in pathways similar to those revealed by the transcriptome analysis, particularly tolerance-inducing pathways and cell signaling genes, stressing the importance of histone marks in T cell function.

Materials and Methods

Cell purification and stimulation

Neonatal blood was collected from the umbilical cord vein of healthy full-term neonates, born through vaginal delivery at Hospital General Parres (Cuernavaca, Morelos, Mexico), with full informed consent from the mothers and the ethical approval of the hospital (CONBIOÉTICA-17-CEI-001-20160329). Adult cells were obtained from Centro Estatal de la Transfusión Sanguínea, Cuernavaca. The permission to use blood samples was given by Servicios de Salud Morelos, through the establishment of an official agreement (File 1372/1706). To ensure that cord blood represents the baby's blood, we obtained the samples before the placenta expulsion, to avoid mixing with the mother's blood and the presence of coagulation factors, which changes the proportion of the cells and the serum in the samples. A routine evaluation of the purity of all samples and the absence of $CD45RO^{hi}$ cells was performed to ensure that no contamination with the mother's blood occurred.

Samples were processed the same day to obtain mononuclear cells by density gradient centrifugation using Lymphoprep (Axis-Shield; Dundee, UK) and cultured overnight in tissue culture dishes (Corning 353003) to eliminate adherent cells. $CD4^+$ T cells were isolated from mononuclear cells using the RosetteSep $CD4^+$ T cell enrichment cocktail (STEMCELL), with 1 ml of erythrocytes from the same blood sample, kept in culture for one day, and used in a second density gradient. Memory and effector cells were eliminated from adult blood with magnetic beads (Pierce) coupled to anti-CD45RO (UCH-L1, TONBO biosciences; California, USA) and anti-CD44 (IM7, TONBO biosciences; California, USA) antibodies that depleted the $CD44^{hi}$ and CD45RO populations. Purification of neonatal cells also required further depletion of $CD11b^+$ cells with magnetic beads to eliminate contaminating precursor cells, including precursor B cells, NK cells and myeloid precursors that are positive for this marker (20-24). Of note, naïve T cells do not express CD11b. Because both neonatal and adult cells were submitted to antibody depletion with magnetic beads, the purification procedure took the same time and the same steps. Naive cells were cultured in RPMI medium (Thermo Fischer Scientific; Massachusetts, USA), supplemented with 5% de fetal bovine serum (FBS), 1% glutamine, and antibiotics (100 U/ml penicillin and 100 µg/ml streptomycin) at 37°C and 5% de CO2. The purity of our populations of $CD4^+CD3^+CD45RO^-$ cells was 93%, using CD4 (20-0048-T100, TONBO biosciences) and CD3 (20-0037-T100, TONBO biosciences)(Suppl. Figure 1 panels A and B) . The culture Tissue Culture Dishes used were from Corning, maintaining a cell concentration at 3 to 5 X 10^6 cells/ml. Cells were stimulated by crosslinking CD3 and CD28 with a secondary antibody.

RNA preparation and sequencing

RNA was prepared using Trizol (Thermo Fisher Scientific; Massachusetts, USA 15596-018, Invitrogen), following the manufacturer's instructions. Purified RNA was analyzed for integrity with a Bioanalyzer nano-RNA-Kit (Thermo Fisher Scientific; Massachusetts, USA)

and only samples with an integrity value (RIN) above 8.0 were used. Three neonatal and three adult cells samples were sequenced in Transcriptomic and Genomic Platform Marseille Luminy, in France, using the NextSeq-500 Sequencer Illumina (20-120Gb). The reads were generated from Illumina Hiseq.

Data Analysis

Data quality was evaluated using the FASTQC program (25). Adaptors and low-quality reads were cut using Trimmomatic (26) version 0.39 with the following parameters: "ILLUMINACLIP:Truseq3-SE:2:30:10 TRAILING:3 MINLEN:40"9. The reads were aligned against reference transcriptome GRCh38/hg38, using the STAR 2.4.2[a] software with the following parameters: "runMode alignReads -outSAMtype BAM SortedByCoordinate -outFilterMultimapNmax 1"10. The BAM (Binary Alignment Map) files generated by alignment were visualized in regions of interest with IGV (27). Read counts per gene were obtained using the software HTSeq-count (28). To identify differentially expressed genes, we used the DESeq2 package in R (Bioconductor) (29). An adjusted p-value ≤ 0.05, with a log fold change ≥ 1 was considered for differentially expressed genes, which were used for functional annotation. To evaluate the overexpressed pathways, we used the ClusterProfiler in R, using the function EnrichKEGG, and the KEGG pathways (Kyoto Encyclopedia of Genes and Genomes). Enriched pathways were visualized using enrichplot (Bioconductor). To amplify our search for enriched pathways, we used the stringAPP from Cytoskape.

Flow cytometry

Neonatal and adult $CD4^+$ T cells were purified, and gene expression was assessed with specific antibodies. The experimental gating strategy is illustrated in Suppl. Fig. 1.

A selection of differentially expressed genes was evaluated by flow cytometry with antibodies targeting BCL11A (MA5-34678, Thermofisher), CEBP-alpha (aEbs-1630R, Thermofisher), GLUT1 (sc-377228 AF790, Santa Cruz Biotechnology), HOXA3 (PA5-56077, Thermofisher), HOXA9 (PA5-102516, Thermofisher), INSR (sc-57342 AF790, Santa Cruz Biotechnology), DUSP6 (MA5-31988, Thermofisher), together with the secondary antibody Goat anti-Rabbit IgG FITC (35-8067, TONBO). Protein expression was evaluated in an Attune cytometer (Life Technologies) and analyzed using the Flow-Jo X software. The flow cytometry strategy for protein expression is shown in Suppl Figure 6.

Evaluation of proliferation and early activation in response to TCR/CD28 signals

For assays of cell division, mononuclear cells from neonate and adult donors were left untreated or activated by crosslinking CD3 (70-0037-U100, TONBO) and CD28 (70-0289-U100, TONBO) with a second antibody (Goat Anti-Mouse IgG Antibody (H+L) bs-0296G, Bioss Antibodies). Dividing cells were specifically evaluated by double staining with CFSE

(21888, Sigma) 50 nM and CD4-PerCP-Cyanine 5.5 (65-0048-T100, TONBO). Dilution of CFSE on the $CD4^+$ gate was measured after incubation for 96 h in an Attune cytometer (Life Technologies) and analyzed using the Flow-Jo X

Early activation response from neonatal and adult $CD4^+$ T cells was assessed by transcriptome analysis of the same cells, after crosslinking CD3 and CD28 with a secondary antibody Goat Anti-Mouse IgG Antibody (H+L) (bs-0296G, Bioss Antibodies) for 6 h. Gene expression was performed as indicated previously.

Chromatin states and chromatin marks levels

We used ChIP-seq data of chromatin marks (H3K4me3, H3K4me1, H3K27ac, H3K27me3, H3K36me3, H3K9me3) from three naive ($CD45RA^+$) neonatal $CD4^+$ T cell and four naive ($CD45RA^+$) adult $CD4^+$ T cell samples made available by the BLUEPRINT consortium. The primary analysis was performed by BLUEPRINT consortium, and the peaks (bed files) and coverage files (bigwig files) were downloaded from their latest release (2016) for further analysis.

ChIP-seq peaks of histone modifications were given as input to the software ChromHMM (http://compbio.mit.edu/ChromHMM/) to segment the genome in different regions (200bp) and computed a 12-state model of chromatin states (with the parameters BinerizeBed –center option, assembly hg38; LearnModel 12 states). Using the ChromHMM results, we then selected the regions (states) associated with marks of active promoters ($H3K4me3^+H3K27ac^+H3K4me1^+$; state 12) and enhancers ($H3K4me1^+H3K27ac^+$; state 9), which were annotated using the software GREAT (http://great.stanford.edu/public/html/). GREAT assigns a regulatory domain to each gene, and then annotates each genomic region given (query regions) to a gene (or genes) whose regulatory domain it overlaps. We annotated our active promoter regions (state 12) by selecting the single nearest gene to our regions (states), whose domain extends within +/- 2kb around the transcription start (TSS), while active enhancer regions (state 9) were annotated by selecting the single nearest gene to our regions, whose domain extends +/- 100kb of the TSS. Then, using the list of genes annotated to states 12 and 9 in neonatal and adult cells, we generated a Venn diagram to identify the genes exclusively annotated to one type of regulatory region (state 9 or 12) generating 4 unique gene lists. Then, we performed the functional annotation analysis for the 4 gene lists using EnrichKEGG. This strategy is illustrated in Suppl. Fig. 8.

To gain a more quantitative comparison at the level of promoters, we extracted the chromatin marks scores for the regions within +/- 2kb from the start of each differentially expressed gene, as a measure of the intensity of the mark in the promoter region. For this, we used the coverage (bigwig) files from BLUEPRINT consortium and the software deepTools (https://deeptools.readthedocs.io/en/develop/). Once we obtained the levels of four chromatin marks (H3K4me3, H3K4me1, H3K27ac, H3K27me3) in the promoter regions of the differentially expressed genes, we performed the statistical analysis to compare the level of each mark in adult and neonatal cells using R.

Association of SNPs identified by GWAS with active enhancers and promoters enriched in the adult or neonatal cells.

To further explore the potential function of regulatory regions enriched in the neonatal and adult $CD4^+$ T cells, we aligned SNPs identified in 413 GWAS studies, obtained from the [IEU OpenGWAS project] (https://gwas.mrcieu.ac.uk/), with the DNA regions corresponding to active promoters and enhancers from our ChromHMM analysis in neonatal and adult cells. The 413 GWAS were selected based on these four criteria: i) molecular phenotypes such as proteome or methylome were excluded; ii) only studies from the European population were kept because more studies are available, and our epigenetic data came from Europeans; iii) only well-defined medical or physiological conditions were kept and environmental phenotypes such "employment status" or "self-reported" medical conditions were excluded; iv) only GWAS studies with at least 10000 subjects, 2000 controls, and 2000 cases were kept.

To compare active promoter and enhancer-enriched regions in neonatal versus adult cells with regions associated with diseases in GWAS studies, we implemented the following workflow:

1. Unique peaks in the two sets of peaks were computed.

2. These unique peaks were binned in windows of 500 nt.

3. For a list of 413 GWAS (Supplementary table 2) from the [IEU OpenGWAS project] (https://gwas.mrcieu.ac.uk/), the number of peaks with and without significant GWAS signals was counted.

4. A statistical Fisher test was used to evaluate the significance of the counting in the two sets of peaks with and without GWAS signals.

5. The results of the 413 GWAS were concatenated, and a Bonferroni multi-test correction was applied.

Results

Neonatal CD4+ T cells have a unique transcriptome

$CD4^+$ T cells coordinate adaptive immune response and are crucial for the activation of other immune cells and a good antibody response. In neonates, however, $CD4^+$ T cells have a high threshold of activation and a low effector function (7-9, 30, 31). To better understand the functionality of these cells, we performed RNA-seq analysis of $CD4^+$ T cells purified from cord blood, as compared to naive adult cells. In both cases, blood was processed within hours of collection. Cord blood was obtained immediately after birth before the placenta was expelled. Three samples of neonates and adults were processed for transcriptome sequencing, and after aligning the reads to the human genome (GRCh38), we obtained 60,676 transcripts annotated in Ensembldb (Rainer et al., 2019), and a total of 1,999 differentially expressed genes (DESeq2; p-adj < 0.05 and a log2FoldChange >= 1) (Supplementary Table 1). Among these genes, 862 and 1137 were found overexpressed genes in adult and neonatal cells, respectively.

A PCA analysis revealed that the neonatal and adult samples separated well from each other, indicating they have specific transcriptome signatures, which is illustrated in the volcano plot (Figure 1, panels A and B).

The functional annotation of the differentially expressed genes was performed with EnrichKEGG (ClusterProfiler), using the KEGG database (Kyoto Encyclopedia of Genes and Genomes). Seven pathways were associated with overexpressed genes in the neonatal cell samples with a p-adj< 0.05 (Figure 1C), while the overexpressed genes in adult cells were not significantly enriched in any pathway. We performed a second analysis to search for pathways in the adult populations with the STRING application in Cytoskape. Again no pathways were found enriched in the adult cells' overexpressed genes. The genes overexpressed in the neonatal cells form a big network (Suppl. Figure 4), in contrast to adult overexpressed genes, which were dispersed and only form small networks (Suppl.Figure 5). The pathways enriched in the neonatal (Figure 1D were *Transcriptional Misregulation in Cancer*, which includes genes with regulatory functions (*FLT1, PLAU, HPGD)* (32-34), genes overexpressed in hematopoietic and immature T cell precursors, several of them related to hyperproliferation and T-ALL (*PROM1, HOXA9, HOXA10, PDGFA, MYCN, LMO2, PMP2K, MEIS1, HMGA2, HHEX, ERG, H3C10*) (35); genes typically associated with neutrophils and antimicrobial activities (*MPO, ELA, DEFA3, DEFA4*); as well as cell signaling genes (*DUSP4, DUSP6, TSPAN, SLC453, AMS1, JUP, RXRA, NTRK1*), particularly with regulatory functions. The *Central Carbon Metabolism in Cancer* and *HIF1* pathways are enriched in aerobic glycolysis enzymes, such as *LDH*, *HK1,* and *HK2*. The Focal adhesion and platelet activation pathways are involved in cytoskeleton rearrangements and cell migration, which in agreement with the enrichment *Rap Signaling Pathway*, controls cell migration and cytoskeleton rearrangements. Finally, the *RAS Signaling Pathway* controls cell proliferation, which, together with the hyper-proliferation genes previously described, suggest that neonatal cells are engaged in homeostatic proliferation.

In Suppl. Figure 2A, we represent the 50 genes that showed the highest differences between neonatal and adult cells, and in panel B, we show the differentially expressed top 60

transcription factors). The genes overexpressed in neonatal cells are involved in the cytoskeleton, cell adhesion and migration (*MROCK1 CD93, MTSS2, FBLN2, KDR1*), control of cell signaling (*PDE6G, PTPRD*) and development (*NREP, AUTS2, IGR2BP3*). The genes overexpressed in adult cells are more involved in cell function (*TMEM3OB, PLEKHH2, SGSM1, KIF5C, KIF21A, FLT4*) and genome structure and stability (*RADX, NAP1L2, TCEAL2*). The transcription factors differentially expressed between neonatal and adult cells are shown in panel 3B. Many of the neonatal cells' transcription factors are involved in development and hyperproliferation. Among these, we found *ZFN423*, which has been related to DNA damage repair (36); *BCL11A*, an important regulator of early lymphopoiesis, also involved in chromatin remodeling through its association with the SWI/SNF (37); *TOX,* which is involved in the maturation of T cells and in the inhibition of effector functions, driving also T cell exhaustion (38). Also remarkable is the expression of the homeobox genes, *HOXA* and *HHEX*, which are involved in developmental processes (39), HOXA3 is particularly involved in thymus development (40). *CEBPA* codes for a transcription factor controlling enhancer expression and function and regulates proliferation (41). In contrast, the Transcription Factors overexpressed in adult cells are related to typical T cell function, such as T-bet (*TBX21*), the EOMES transcription factors, and STAT4, which is activated in response to IL-12 and is involved in Th1 differentiation. We also compared the differential expression gene profile in our transcriptome, with RNA-seq data from neonatal and adult cells in the BLUEPRINT database. We can see that the differential genes are similar between the samples, validating our statistically significant results.

Protein expression, proliferation, and early activation in response to TCR/CD28 signals

To confirm our transcriptome results, we evaluated the protein expression of several genes overexpressed in neonatal cells by flow cytometry, among the live cells-gate, and among the $CD31^+$ cells, to exclude that the observed differences could result from a different proportion of Recent Thymus Emigrants in neonatal and adult cell populations. The gating strategy to analyze CD31 is shown in Suppl. Figure 1C and Suppl. Figure 6. CD31 is a marker accepted for Recent Thymus Emigrants in $CD4^+$ T cells (42). The adult T cells came from young adults, aged 20 to 30 years old, and CD31 expression was similar between neonatal and adult cells (Suppl. Figure 3). We found that the seven proteins evaluated were significantly increased in the neonatal cells, and the analysis on the $CD31^+$ population did not change the general protein expression profile (Figure 2A).

Next, we evaluated neonatal and adult $CD4^+$ T cell proliferation by CFSE dilution (the gating strategy to analyse proliferation is shown in Suppl. Figure 7. In agreement with the transcriptome profile, the neonatal cells proliferated more (Figure 2B), both without stimulation (homeostatic proliferation) and after CD3/CD28 signals (Activation-induced proliferation). Neonatal cells generated up to two generations without stimulus (Figure 2D), and up to three generations after activation (Figure 2C), while the adult cells did not divide homeostatically, with only a small proportion of the cells reaching one division after activation with no cytokines added to the medium.

We then evaluated the transcriptome of early activated neonatal and adult CD4+ T cells. After 6 h of incubation with CD3/CD28 signals, cells were collected, and differential gene

expression analysis was performed. In neonatal cells, only one gene was found downregulated, while 75 genes were overexpressed after cell activation. In contrast, in adult cells, 53 genes were downregulated, while 287 genes were upregulated, under the same activation conditions (Figure 3A). The top 80 differentially expressed genes in neonatal and adult cells upon activation are shown in Suppl. Figure 8. The comparison between activated neonatal and adult cells showed 1,457 genes overexpressed in the neonatal cells, and 1,083 genes in the adult ones (Figure 3A). An analysis of KEGG pathways enrichment (Figure 3B) revealed an upregulation of metabolic, adhesion, and movement pathways upon activation in neonatal cells (see middle column), while in the adult cells both T cell receptor and innate receptor pathways were upregulated (see right column of Figure 3B), outlining the activation of the cells and suggesting an important function of Toll and NOD receptor pathways in naive cell activation, as we previously reported for TLR5 (43, 44).

An Epigenetic signature of neonatal CD4$^+$ T cells

To better understand neonatal CD4$^+$ T cells, we compared the epigenetic landscape of the neonatal and adult cells. For that, we used Chromatin Immunoprecipitation data (ChIP-seq) from the Blueprint Consortium (https://www.blueprint-epigenome.eu/) for human neonatal and adult naive CD4$^+$ T cells. We analyzed six different chromatin mark profiles, including H3K27ac, H3K4me3, and H3K36me3 denoting open chromatin, H3K27me3 and H3K9me3 denoting closed chromatin, and the enhancer mark H3K4me1. We then used the ChromHMM software to compute chromatin states representing the chromatin regions involving specific combinations of the different chromatin marks (Figure 4A). We generated a 12-state chromatin model and focused on the active enhancers state (state 9) marked in violet and active promoters (state 12) marked in yellow (Figure 4B). The changes in active promoters, bimodal regions, and active and inactive enhancers between neonatal and adult cells are also indicated (Figure 4C). Interestingly, the biggest changes occurred at the level of enhancers and bimodal regions.

We then used IGV to visualize the RNA-seq signal associated with the regulatory regions of the genes. Figure 6 shows four selected genes, *INSR* and *GLUT1,* which are highly expressed only in neonatal cells, *HK2*, which is expressed in both neonatal and adult cells but overexpressed in neonates, and *CAMK2N1,* which is overexpressed only in adult cells, displaying the active enhancer (purple squares) and active promoter (yellow squares) states in their regulatory regions. Interestingly, some genes overexpressed in neonates were associated with active promoters and enhancers that were not active in their adult counterparts. In other cases, such as *HK2*, although active promoters are present in both neonate and adult cells, additional active enhancer regions are present in neonatal cells, possibly inducing a higher expression. In the case of *CAMK2N1,* overexpressed in adult cells, the active promoter state is found only in the adult cells (yellow) (Figure 6 D-G). The visualization of the HOX cluster expression peaks and its regulatory regions is shown in Suppl. Figure 9.

To further understand the potential function of regulatory regions enriched in the neonatal and adult CD4$^+$ T cells, we aligned the chromatin regions enriched that were designated as active enhancers or active promoters in our ChromHMM analysis with SNPs identified in

413 GWAS studies, obtained from the IEU OpenGWAS project,. We found a significant enrichment of SNPs associated with Rheumatoid arthritis and asthma in the adult cell active promoters, in agreement with the typical high activation profile of the adult cells. No correlation was found in the neonatal promoters with GWAS data. In contrast, two hits were found in the active enhancers of neonatal cells with prostate cancer, in agreement with the high expression of the HOX genes and the higher proliferative profile of these cells. No correlations were found in the adult cells' enhancers (Figure 4H).

We next focused on the active enhancers and active promoters (states 9 and 12, respectively) to obtain proximal genes, exclusive for either neonatal or adult cells. Suppl. Figure 10A displays the enhancer and promoter regions of neonatal and adult cells, showing very few shared regions, with the number of regions associated with each of them. Suppl. Figure 10B, shows the top 20 pathways enriched with the genes associated with enhancers of neonatal cells, while no pathways were associated with adult cells. Among the pathways enriched in neonatal cells, we found overrepresented the PD-L1-PD1 pathway, which has been reported as a master regulator of tolerance in tumor microenvironments (45), as well as the senescence pathway, also associated with immunosuppression. Anti-viral response pathways and other pathways already revealed by the transcriptomic signatures were also enriched, including the HIF pathway and proliferation. TCR signaling genes were also found associated with active enhancers, including positive and negative signal receptors (*CD3, CTLA4,* and *PD-1*). Genes involved in AP-1, NF-κB, and NFAT activation, as well as in NOD pathways were also found enriched.

To gain insight into the role of each mark in the epigenetic landscape of neonatal and adult genes, we extracted the enhancer (H3K4me1), chromatin opening (H34K4me3 and H3K27ac) and repression (H3K27me3) marks levels in the promoter regions (+/- 2kb from the gene start) of adult and neonatal specific genes. Figure 5A shows the presence and and distribution of the marks along the gene promoters in neonatal signals. The neonatal cells present slightly higher levels of the opening marks H3K4me3 and H3K27ac, with a slight reduction in the closed chromatin mark H3K27me3. This mark is difficult to visualize because of its broad presence along the genes. In the adult cells' overexpressed regions (Figure 5B), we found higher levels of the H3K4me3, H3K4me1 and H3k27ac open chromatin marks, and a much lower level of the H3k27me3 closed chromatin mark. When we evaluated the average levels of the marks in promoters of neonatal overexpressed genes the only significant difference involved the closing mark H3k27me3, which was slightly lower in neonatal cells. In the genes overexpressed in adult cells, changes were significant for all the marks, but the closed chromatin mark was remarkably much higher in the neonatal cells. This suggests that during the maturation of neonatal cells toward the adult epigenome, gene promoters lose neonatal-enriched closed chromatin marks and open the adult-enriched regions and that the regulation of H3K27me3 mark is very important for this change.

Finally, in Figure 6, we present a summary of the main conclusions of our study, showing that neonatal cells are characterized by a specific epigenetic and gene expression profile, pointing to particular physiological adaptations, which should be considered in the design of vaccines or therapeutical strategies targeting the neonatal immune response.

Discussion

Our study provides a thorough characterization of the unique transcriptome of neonatal $CD4^+$ T cells. The main signature of the neonatal cell transcriptome is the expression of genes associated with regulatory functions, proliferation, migration, aerobic glycolysis, antimicrobial activities, and regulation of cell signaling. The transcriptome results were confirmed by changes in protein expression in basal conditions, proliferation, and changes in gene expression upon activation.

Our data demonstrate the high expression of three important genes associated with a regulatory function in neonatal $CD4^+$ T cells: the gene *FLT1*, which is related to a new subset of T regulatory cells, as well as *PLAU* and *HPGD* genes, also implicated in suppressor activities (32-34). Our study reveals a characteristic expression of transcription factors in neonatal cells, with overexpression of master regulators of chromatin structure, including ZFN423, which has been related to DNA damage repair (36), Bcl11a transcription factor, which binds the SWI/SNF chromatin remodelers (37). CEBPA is a transcription factor controlling enhancer expression and function, metabolism, proliferation, and myeloid cell development (41).

The gene coding for the transcription factor TOX was also found overexpressed in the neonatal samples. TOX is a master negative regulator of effector functions, reported for T cell exhaustion (38). In agreement with a rather tolerant response, the gene expression after T cell activation was much lower in the neonatal as compared with adult cells and was not a typical T cell response. Yet, the proliferation response was higher in the neonatal cells. This is in agreement with the high expression of hyperproliferative genes in neonatal $CD4^+$ T cells, particularly those coding for the family of HOXA transcription factors. HOXA factors play a key role in controlling cell identity and differentiation of HSCs and T cell progenitors (46, 47). Progressive down-modulation of HOXA transcripts has been reported during thymic cell maturation (35, 48), while sustained expression of HOXA genes during T cell differentiation has been shown to impair T cell maturation and induce oncogenic transformation (35). Therefore, the maintained expression of these genes in neonatal T cells might impose an "immature" epigenetic state contributing to the more tolerant immune response phenotype of these cells.

Metabolism is an important determinant of immune function, and determine effector and memory cells differentiation. In our study, we found that the expression of metabolic genes was altered in the neonatal cells, with a high expression of glycolytic enzymes. Glycolysis and oxidative phosphorylation (OXPHOS) are the two main cooperative processes that supply ATP within the cell. When pyruvate is fermented to lactate in the cytoplasm, even when sufficient oxygen is present to utilize OXPHOS, a process known as the Warburg effect occurs, also known as aerobic glycolysis, which is characteristic of rapidly dividing cell types (49). We found that neonatal $CD4^+$ T cells overexpress Glucose Transporter Type 1*(SLC2A1*) and genes involved in aerobic glycolysis (*HK1, HK2, LDHA*), as well as genes from the HIF-1 signaling pathway. The HIF-1 signaling pathway has been reported to enhance glycolysis in tumor cells (50). HIF is also a sensor of hypoxia, which could be associated with vaginal delivery. This could be a caveat of our study, however, our protocol for cell purification took 2 days, in which neonatal and adult cells were under the same normoxic conditions. During this time most of the stress- and hypoxia-related genes should have faded away, such as the

HIF gene itself, which was not overexpressed in the neonatal samples. We also found the overexpression of the monocarboxylate transporter gene (*SLC16A3*), which functions in L-lactate export and is highly expressed in glycolytic and anaerobic tissues (51). Our results suggest that neonatal $CD4^+$ T cells have a metabolic program dependent on aerobic glycolysis. Neonatal $CD4^+$ T cells could be using aerobic glycolysis to divert the use of glucose for the biosynthesis of macromolecules that will be used for proliferation.

Migration and cytoskeletal changes in the neonatal cells are expected, as these cells will not only go to lymph nodes but also colonize mucosal tissues. Expression of genes involved in the migration to the mucosa in unstimulated cells was also observed in the unstimulated neonatal $CD8^+$ T cells (18).

We found a regulatory bias on the neonatal $CD4^+$ T cells, and even more so associated with activated enhancers. This regulatory bias was also observed on expanded cord blood $CD4^+$ T cells as compared with similarly treated adult cells, mostly towards regulatory Th17 cells, with a lower expression of IL 17 and its signature transcription factor RORγT, and a higher expression of FoxP3 (52). An immunoregulatory IL-22-dominated Th17 profile was recently published for neonatal CD4+ T cells, apparently due to differences in the TGF-β signaling pathway (53). Remarkably, we found the Th17 pathway enriched close to open enhancers in neonatal cells. It will be interesting to further explore this pathway.

The transcription factors overexpressed in adult cells are related to typical T cell function, such as the T-bet (*TBX21*) and STAT4, the Th1 signature transcription factors, and EOMES, which marks memory cells. The presence of these factors does not imply that cells are not naive but that the basal expression, due to the open chromatin in the adult naive cells, may prepare them to effector or memory differentiation, particularly the Th1 profile.

The unique transcriptome of the neonatal $CD4^+$ T cells is further accompanied by a characteristic epigenomic landscape. Overexpressed genes in adult cells have higher levels of open chromatin marks, H3K4me3, H3K4me1, and H3K27ac in their promoter regions, with a significantly lower level of the closed chromatin mark H3K27me3. In contrast, upregulated genes in neonatal cells have slightly higher levels of open chromatin marks, with a slight but significant difference in the closed chromatin mark H3K27me3. This suggest that the change of neonatal towards adult cells involves a fine regulation of histone marks, particularly H3K27me3. A potential caveat of this study is the origin of the samples used for transcriptome analysis (Mexican population and young adults) and the European population for the epigenomic data and the SNP analysis. However the transcriptomic and epigenetic analysis results are in agreement with each other, suggesting that the profiles shown are not particular for a human ethnia, but broad to all humans.

Combining the chromatin marks analyzed, we defined 12 chromatin states and visualized the mean peaks corresponding to promoters and enhancers of selected genes, and found that these states corresponded with the level of expression of the genes. Overexpressed genes in neonatal cells are associated with intergenic active enhancer regions (H3K4me1+H3K27ac+). The functional analysis of the corresponding genes led us to identify 146 enriched pathways. Some of these pathways were the same as in the transcriptomic signature. Cancer-related pathways, presumably related to the overexpression of the hyperproliferative genes, were also found in genes close to the active enhancers. We also found a strong enrichment in pathways related to tolerance and the regulatory Th17

pathway. The epigenetic landscape expands the transcriptome analysis, which shows what is happening in the cells in a precise moment, to the readiness of the cells to respond in particular ways. In this way, both functional annotations are not expected to be identical.

We have previously published the transcriptomic and epigenomic analysis of neonatal $CD8^+$ T cells (16). Several characteristics are shared in the neonatal $CD4^+$ T cells, such as cell cycle, antiviral response pathways, and antimicrobial peptides expression, but there are also important differences. Specifically, in neonatal $CD4^+$ T cells, genes of the TCR signaling pathway were associated with active enhancers, which suggests that $CD4^+$ T cells are readier to activate cell signaling upon the proper maturation stimuli. Negative signaling is also more strongly associated with the $CD4^+$ T cells, including exhaustion-like gene expression (PD-1/PD-L1, cellular senescence, apoptosis, necroptosis). Another difference consists in the higher proliferation of neonatal $CD4^+$ T cells in response to stimulation, which was not found in the $CD8^+$ T cell population. Remarkably, neonatal $CD4^+$ T cells appear to be ready to activate all cell functions, while they have strong regulatory regions. It could be very interesting to find which signals regulate the expression of either group of genes.

In any case, our data shows that neonatal $CD4^+$ T cells have a unique transcriptomic and epigenomic signature, enriched in glycolysis-, proliferation- and tolerance-related genes, that predisposes them to lower immune responses. In a recent single cell sequencing study, it was shown that the transition of human fetal to adult T cells it was found that cells evolve in a progressive way, rather than in waves, suggesting that the neonatal T cells mature into adult cells (54) and are not a unique population that is replaced by the adult-like cells. In a different study, it was shown that immune cells follow a stereotypic developmental pattern towards the adult-like cells (55) We found that histone marks, particularly H3K4me3 are important in the establishment of the unique genomic structure of neonatal cells. Several enzymes participating in the methylation of this particular histone mark have been found (56). It will be interesting to characterize these enzyme functions in the neonatal T cells.

Legends to figures

Figure 1. Differentially expressed genes between unstimulated naive neonatal and adult $CD4^+$ T cells. A) Principal components analysis showing naïve neonatal and adult cells. B) Volcano plot displaying the differentially expressed genes in basal adult vs. neonatal $CD4^+$ T cells C) Functional analysis of pathways enriched in neonatal cells overexpressed D) Network showing the connections between the neonatal overexpressed genes of these different pathways

Figure 2: Changes in protein expression and proliferation assays. A) Protein expression in unstimulated cells was evaluated by intracellular flow cytometry in the general living cells gate and in the CD31+ cell gate. B) Proliferation of neonatal (blue) and adult (red) cells without any stimulus (homeostatic proliferation) or after stimulation by crosslinking CD3 and CD28 for 96 h (activation induced proliferation). Frequency of cells by the number of divisions in samples after stimulation (C) and without stimulation (D).

Figure 3. Gene expression analysis of neonatal and adult $CD4^+$ T cells after stimulation with CD3/CD28 signals. (A) Venn diagrams show the number of differentially expressed genes upon stimulation in neonatal (blue) or adult (red) cells. (B) Functional annotation of the differentially expressed genes showing the enriched Kegg Pathways.

Figure 4. Epigenetic landscape of the neonatal and adult $CD4^+$ T cells. (A) Chromatin states were computed with the software ChromHMM. (B) Color code for the ChromHMM states. (C) Changes in the regulatory states between neonate and adult cells. (D -G) Genomic tracks for four selected genes overexpressed in neonatal cells or overexpressed in adult cells, with their chromatin state annotations. (H) Assignation of SNP-associated diseases, from 413 GWAS studies to neonatal or adult regulatory regions classified as active promoters or enhancers, from our ChromHMM analysis.

Figure 5. Histone marks in promoter regions of genes overexpressed in neonatal or adult $CD4^+$ T cells. Representative histone mark profiles (H3K4me3, H3K4me1, H3K27me3, and H3K27ac) in promoter regions (around TSS) of genes overexpressed in neonatal (A) and adult cells (B), showing the average of the distribution of the mark in the promoters of the genes (left columns) and the average presence of the mark in the adult (A) and neonatal (N) cells. ChIPseq data was obtained from the BLUEPRINT consortia.

Figure 6. Graphical summary of the main differences found in neonatal versus adult T CD4+ cells. Arrows represent the enrichment of each profile, either in unstimulated cells (Basal) or after CD3/CD28 signals. The number of arrows indicate the enrichment strength of each of the pathways. Arrows pointing upwards indicate that the pathway is enriched, and downwards if it is downregulated, in the comparison between neonatal and adult cells.

Supplementary Figure 1: Flow cytometry figures of purity and CD31 analysis. A) Representative figure of cell purity. B) Elimination of CD45RO cells C) Gating strategy for the analysis of CD31.

Supplementary Figure 2: Heatmaps of differentially expressed genes. A) Top 50 differentially expressed genes B) Top 60 differentially expressed transcription factors

Supplementary Figure 3: CD31 expression in neonatal and adult cells. A)Representative flow cytometry of adult and neonatal cells CD31 expression. B) Boxplots of percentage of CD31+ cells.

Supplementary Figure 4: protein networks of genes overexpressed in neonatal cells, generated and analyzed using the STRING app in Cytoskape. To generate this network, only high confidence functional interactions reported in STRING database were taken into consideration. The intensity of the blue color represents the fold change while the size of the node represents the significance (FDR).

Supplementary Figure 5: Protein networks of genes overexpressed in adult $CD4^+$ T cells, generated and analyzed using the STRING app of Cytoskape. To generate this network, only high confidence functional interactions reported in STRING database were taken into consideration. The intensity of the red color represents the fold change while the size of the node represents the significance (FDR).

Supplementary Figure 3: Heatmaps representing the top differentially expressed genes of neonatal (A) and adult (B) T cells upon activation for 6h with CD3/CD28 signals.

Supplementary Figure 4. Visualization of the expression and chromatin states in the HOXA gene cluster using IGV.

Supplementary Figure 5: A) Identification of unique genes associated with active enhancers or promoters for each cell type according to ChromHMM states 9 and 12, respectively. A Venn diagram was drawn with four lists of genes associated with active enhancers and promoters in adult and neonatal CD4+ T cells. The gene – region association was performed using the GREAT tool. B) Top 25 pathways found significantly enriched for Enh N genes using clusterProfiler. Enh N: Genes associated with active enhancers in neonatal cells. Enh A: Genes associated with active enhancers in adult cells. Prom N: Genes associated with active promoters in neonatal cells. Prom A: Genes associated with active enhancers in adult cells.

Supplementary Figure 6: Gating strategy for flow cytometry analysis. A) CD31+ population was selected from a biaxial dot plot, which was equivalent to the histogram plot. B) Fluorescence Minus One (FMO) controls were generated for FITC and Alexa 790 (AF790). C) Representative figure of the Differentially expressed genes (GDE) are shown in different colors, unstained control is shown in grey and in yellow the secondary antibody control. The analysis was made in neonatal and adult $CD4^+$ T cells.

Supplementary Figure 7: Gating strategy for proliferation analysis.

Supplementary Figure 8: Heatmaps representing the top differentially expressed genes of neonatal (A) and adult (B) T cells upon activation for 6h with CD3/CD28 signals

Supplementary Figure 9: Expression and chromatin states in the HOXA gene cluster.

Supplementary Figure 10 : A) Strategy to select neonatal specific genes associated with enhancers in neonatal cells. B) 25 Top pathways associated with these genes

Supplementary Table 1: Complete list of differentially expressed genes.

Supplementary Table 2: Neonatal cells enriched pathways, analyzed with the StringApp, Cytoskape.

Supplementary Table 3: Gene clusters enriched in neonatal cells, analyzed with the StringApp, cytoskape

Supplementary Table 4: Neonatal cells enriched GO Terms, analyzed with the StringApp, Cytoskape.

Supplementary Table 5: Neonatal cells enriched GO Terms, analyzed with the StringApp, Cytoskape.

Acknowledgments

We thank the blood donors, mothers, babies, and staff of Hospital José G. Parres and Servicios de Salud Morelos for granting access to neonatal blood and leukocyte concentrates. We also thank the Transcriptomics and Genomics Marseille-Luminy (TGML) platform for sequencing RNA-seq samples. TGML is a member of the France Genomique consortium (ANR-10-INBS-0009).

Author Contributions

LAK-C, OR-J, and MAS conceived experiments, analyzed the data, and wrote the manuscript. ORJ and MAS conceived and supervised the project, revised the manuscript, and secured funding. DG-R and CJV-M performed experiments. SS financed the RNA-seq experiments and contributed to the analysis of the data and writing of the manuscript. AG performed the analysis of the alignment of GWAS/SNPs with the regulatory sequences and AM-R and DT provided expertise and feedback.

Funding

Work in the MS and OR-J laboratory was supported by CONACYT grants FC 1690 and CF 2019/1727995. Work in the laboratory of SS was supported by recurrent funding from INSERM and Aix- Marseille University, as well as by funding from INCA (PLBIO018-031 INCA_12619). This work was also supported by ECOS/ANUIES/SEP/CONACYT grant M17S02.

Bibliography

1. Levels and trends in child mortality report [Internet]. 2019.
2. Chen N, Field EH. Enhanced type 2 and diminished type 1 cytokines in neonatal tolerance. Transplantation. 1995;59(7):933-41.
3. Debock I, Flamand V. Unbalanced Neonatal CD4(+) T-Cell Immunity. Front Immunol. 2014;5:393.
4. Rudd BD. Neonatal T Cells: A Reinterpretation. Annu Rev Immunol. 2020;38:229-47.
5. Tsafaras GP, Ntontsi P, Xanthou G. Advantages and Limitations of the Neonatal Immune System. Front Pediatr. 2020;8:5.
6. Glaesener S, Jaenke C, Habener A, Geffers R, Hagendorff P, Witzlau K, et al. Decreased production of class-switched antibodies in neonatal B cells is associated with increased expression of miR-181b. PLoS One. 2018;13(2):e0192230.

7. Mastelic-Gavillet B, Vono M, Gonzalez-Dias P, Ferreira FM, Cardozo L, Lambert PH, et al. Neonatal T Follicular Helper Cells Are Lodged in a Pre-T Follicular Helper Stage Favoring Innate Over Adaptive Germinal Center Responses. Front Immunol. 2019;10:1845.
8. Gans HA, Arvin AM, Galinus J, Logan L, DeHovitz R, Maldonado Y. Deficiency of the humoral immune response to measles vaccine in infants immunized at age 6 months. JAMA. 1998;280(6):527-32.
9. Marshall-Clarke S, Reen D, Tasker L, Hassan J. Neonatal immunity: how well has it grown up? Immunol Today. 2000;21(1):35-41.
10. Siegrist CA. Neonatal and early life vaccinology. Vaccine. 2001;19(25-26):3331-46.
11. Mohr E, Siegrist CA. Vaccination in early life: standing up to the challenges. Curr Opin Immunol. 2016;41:1-8.
12. Gibbons D, Fleming P, Virasami A, Michel ML, Sebire NJ, Costeloe K, et al. Interleukin-8 (CXCL8) production is a signatory T cell effector function of human newborn infants. Nat Med. 2014;20(10):1206-10.
13. Webster RB, Rodriguez Y, Klimecki WT, Vercelli D. The human IL-13 locus in neonatal CD4+ T cells is refractory to the acquisition of a repressive chromatin architecture. J Biol Chem. 2007;282(1):700-9.
14. Palin AC, Ramachandran V, Acharya S, Lewis DB. Human neonatal naive CD4+ T cells have enhanced activation-dependent signaling regulated by the microRNA miR-181a. J Immunol. 2013;190(6):2682-91.
15. Bermick JR, Issuree P, denDekker A, Gallagher KA, Santillan D, Kunkel S, et al. Differences in H3K4me3 and chromatin accessibility contribute to altered T-cell receptor signaling in neonatal naive CD4 T cells. Immunol Cell Biol. 2022;100(7):562-79.
16. Galindo-Albarran AO, Lopez-Portales OH, Gutierrez-Reyna DY, Rodriguez-Jorge O, Sanchez-Villanueva JA, Ramirez-Pliego O, et al. CD8(+) T Cells from Human Neonates Are Biased toward an Innate Immune Response. Cell Rep. 2016;17(8):2151-60.
17. Sanchez-Villanueva JA, Rodriguez-Jorge O, Ramirez-Pliego O, Rosas Salgado G, Abou-Jaoude W, Hernandez C, et al. Contribution of ROS and metabolic status to neonatal and adult CD8+ T cell activation. PLoS One. 2019;14(12):e0226388.
18. Gutierrez-Reyna DY, Cedillo-Banos A, Kempis-Calanis LA, Ramirez-Pliego O, Bargier L, Puthier D, et al. IL-12 Signaling Contributes to the Reprogramming of Neonatal CD8(+) T Cells. Front Immunol. 2020;11:1089.
19. Stunnenberg HG, International Human Epigenome C, Hirst M. The International Human Epigenome Consortium: A Blueprint for Scientific Collaboration and Discovery. Cell. 2016;167(7):1897.
20. Audzevich T, Bashford-Rogers R, Mabbott NA, Frampton D, Freeman TC, Potocnik A, et al. Pre/pro-B cells generate macrophage populations during homeostasis and inflammation. Proc Natl Acad Sci U S A. 2017;114(20):E3954-E63.
21. Cao Q, Huang Q, Wang YA, Li C. Abraxane-induced bone marrow CD11b(+) myeloid cell depletion in tumor-bearing mice is visualized by muPET-CT with (64)Cu-labeled anti-CD11b and prevented by anti-CSF-1. Theranostics. 2021;11(7):3527-39.
22. Crinier A, Narni-Mancinelli E, Ugolini S, Vivier E. SnapShot: Natural Killer Cells. Cell. 2020;180(6):1280- e1.

740 23. Romano L, Seu KG, Papoin J, Muench DE, Konstantinidis D, Olsson A, et al.
741 Erythroblastic islands foster granulopoiesis in parallel to terminal erythropoiesis. Blood.
742 2022;140(14):1621-34.
743 24. Lu W, Cao F, Feng L, Song G, Chang Y, Chu Y, et al. LncRNA Snhg6 regulates the
744 differentiation of MDSCs by regulating the ubiquitination of EZH2. J Hematol Oncol.
745 2021;14(1):196.
746 25. (http://www.bioinformatics.babraham.ac.uk/projects/fastqc.
747 26. Bolger AM, Lohse M, Usadel B. Trimmomatic: a flexible trimmer for Illumina
748 sequence data. Bioinformatics. 2014;30(15):2114-20.
749 27. Robinson JT, Thorvaldsdottir H, Winckler W, Guttman M, Lander ES, Getz G, et al.
750 Integrative genomics viewer. Nat Biotechnol. 2011;29(1):24-6.
751 28. Anders S, Pyl PT, Huber W. HTSeq--a Python framework to work with high-
752 throughput sequencing data. Bioinformatics. 2015;31(2):166-9.
753 29. Love MI, Huber W, Anders S. Moderated estimation of fold change and dispersion
754 for RNA-seq data with DESeq2. Genome Biol. 2014;15(12):550.
755 30. Adkins B, Leclerc C, Marshall-Clarke S. Neonatal adaptive immunity comes of age.
756 Nat Rev Immunol. 2004;4(7):553-64.
757 31. PrabhuDas M, Adkins B, Gans H, King C, Levy O, Ramilo O, et al. Challenges in infant
758 immunity: implications for responses to infection and vaccines. Nat Immunol.
759 2011;12(3):189-94.
760 32. He F, Chen H, Probst-Kepper M, Geffers R, Eifes S, Del Sol A, et al. PLAU inferred
761 from a correlation network is critical for suppressor function of regulatory T cells. Mol Syst
762 Biol. 2012;8:624.
763 33. Schmidleithner L, Thabet Y, Schonfeld E, Kohne M, Sommer D, Abdullah Z, et al.
764 Enzymatic Activity of HPGD in Treg Cells Suppresses Tconv Cells to Maintain Adipose
765 Tissue Homeostasis and Prevent Metabolic Dysfunction. Immunity. 2019;50(5):1232-48
766 e14.
767 34. Shin JY, Yoon IH, Lim JH, Shin JS, Nam HY, Kim YH, et al. CD4+VEGFR1(HIGH) T cell
768 as a novel Treg subset regulates inflammatory bowel disease in lymphopenic mice. Cell
769 Mol Immunol. 2015;12(5):592-603.
770 35. Cieslak A, Charbonnier G, Tesio M, Mathieu EL, Belhocine M, Touzart A, et al.
771 Blueprint of human thymopoiesis reveals molecular mechanisms of stage-specific TCR
772 enhancer activation. J Exp Med. 2020;217(9).
773 36. Chaki M, Airik R, Ghosh AK, Giles RH, Chen R, Slaats GG, et al. Exome capture
774 reveals ZNF423 and CEP164 mutations, linking renal ciliopathies to DNA damage response
775 signaling. Cell. 2012;150(3):533-48.
776 37. Kadoch C, Hargreaves DC, Hodges C, Elias L, Ho L, Ranish J, et al. Proteomic and
777 bioinformatic analysis of mammalian SWI/SNF complexes identifies extensive roles in
778 human malignancy. Nat Genet. 2013;45(6):592-601.
779 38. Bordon Y. TOX for tired T cells. Nat Rev Immunol. 2019;19(8):476.
780 39. Alharbi RA, Pettengell R, Pandha HS, Morgan R. The role of HOX genes in normal
781 hematopoiesis and acute leukemia. Leukemia. 2013;27(5):1000-8.
782 40. Manley NR, Capecchi MR. The role of Hoxa-3 in mouse thymus and thyroid
783 development. Development. 1995;121(7):1989-2003.

41. Tada Y, Brena RM, Hackanson B, Morrison C, Otterson GA, Plass C. Epigenetic modulation of tumor suppressor CCAAT/enhancer binding protein alpha activity in lung cancer. J Natl Cancer Inst. 2006;98(6):396-406.
42. Tanaskovic S, Fernandez S, Price P, Lee S, French MA. CD31 (PECAM-1) is a marker of recent thymic emigrants among CD4+ T-cells, but not CD8+ T-cells or gammadelta T-cells, in HIV patients responding to ART. Immunol Cell Biol. 2010;88(3):321-7.
43. Labastida-Conde RG, Ramirez-Pliego O, Peleteiro-Olmedo M, Lopez-Guerrero DV, Badillo-Godinez OD, Gutierrez-Xicotencatl ML, et al. Flagellin is a Th1 polarizing factor for human CD4(+) T cells and induces protection in a murine neonatal vaccination model of rotavirus infection. Vaccine. 2018;36(29):4188-97.
44. Rodriguez-Jorge O, Kempis-Calanis LA, Abou-Jaoude W, Gutierrez-Reyna DY, Hernandez C, Ramirez-Pliego O, et al. Cooperation between T cell receptor and Toll-like receptor 5 signaling for CD4(+) T cell activation. Sci Signal. 2019;12(577).
45. Han Y, Liu D, Li L. PD-1/PD-L1 pathway: current researches in cancer. Am J Cancer Res. 2020;10(3):727-42.
46. Lawrence HJ, Sauvageau G, Humphries RK, Largman C. The role of HOX homeobox genes in normal and leukemic hematopoiesis. Stem Cells. 1996;14(3):281-91.
47. Magli MC, Largman C, Lawrence HJ. Effects of HOX homeobox genes in blood cell differentiation. J Cell Physiol. 1997;173(2):168-77.
48. Taghon T, Thys K, De Smedt M, Weerkamp F, Staal FJ, Plum J, et al. Homeobox gene expression profile in human hematopoietic multipotent stem cells and T-cell progenitors: implications for human T-cell development. Leukemia. 2003;17(6):1157-63.
49. Geltink RIK, Kyle RL, Pearce EL. Unraveling the Complex Interplay Between T Cell Metabolism and Function. Annu Rev Immunol. 2018;36:461-88.
50. Kouidhi S, Elgaaied AB, Chouaib S. Impact of Metabolism on T-Cell Differentiation and Function and Cross Talk with Tumor Microenvironment. Front Immunol. 2017;8:270.
51. Yu S, Wu Y, Li C, Qu Z, Lou G, Guo X, et al. Comprehensive analysis of the SLC16A gene family in pancreatic cancer via integrated bioinformatics. Sci Rep. 2020;10(1):7315.
52. Miyagawa Y, Kiyokawa N, Ochiai N, Imadome K, Horiuchi Y, Onda K, et al. Ex vivo expanded cord blood CD4 T lymphocytes exhibit a distinct expression profile of cytokine-related genes from those of peripheral blood origin. Immunology. 2009;128(3):405-19.
53. Razzaghian HR, Sharafian Z, Sharma AA, Boyce GK, Lee K, Da Silva R, et al. Neonatal T Helper 17 Responses Are Skewed Towards an Immunoregulatory Interleukin-22 Phenotype. Front Immunol. 2021;12:655027.
54. Bunis DG, Bronevetsky Y, Krow-Lucal E, Bhakta NR, Kim CC, Nerella S, et al. Single-Cell Mapping of Progressive Fetal-to-Adult Transition in Human Naive T Cells. Cell Rep. 2021;34(1):108573.
55. Olin A, Henckel E, Chen Y, Lakshmikanth T, Pou C, Mikes J, et al. Stereotypic Immune System Development in Newborn Children. Cell. 2018;174(5):1277-92 e14.
56. Pan MR, Hsu MC, Chen LT, Hung WC. Orchestration of H3K27 methylation: mechanisms and therapeutic implication. Cell Mol Life Sci. 2018;75(2):209-23.

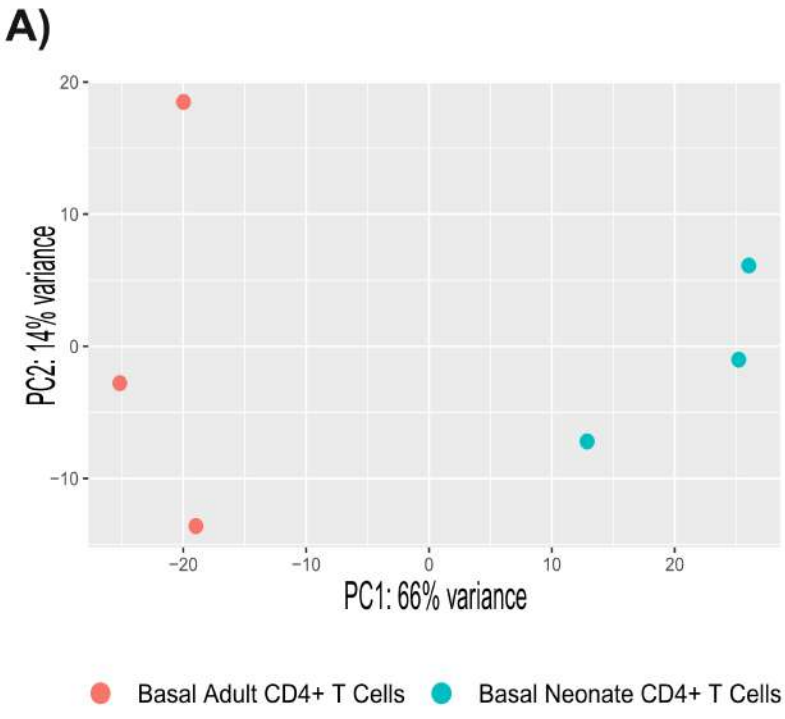
A)
PC2: 14% variance
PC1: 66% variance
Basal Adult CD4+ T Cells
Basal Neonate CD4+ T Cells

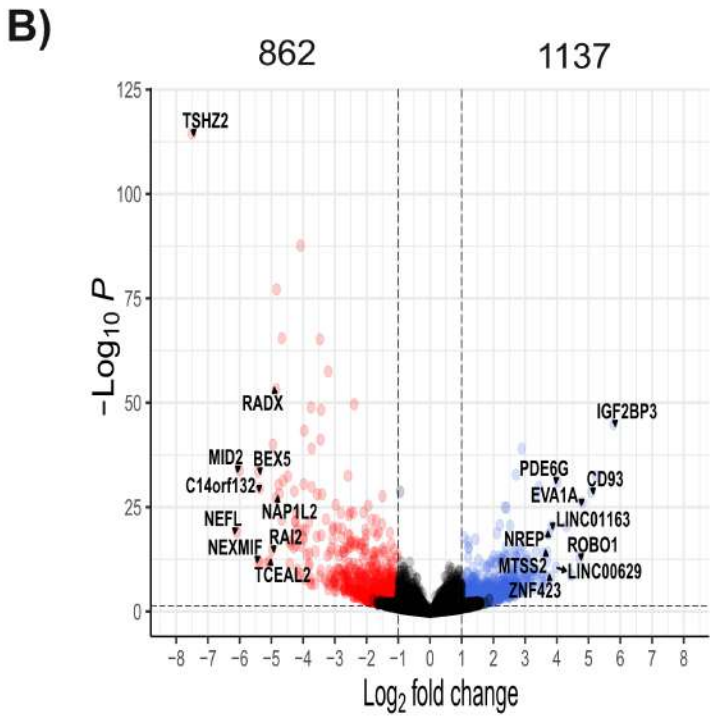
B)
862
1137
TSHZ2
RADX
IGF2BP3
MID2
BEX5
C14orf132
NAP1L2
NEFL
RAI2
NEXMIF
TCEAL2
PDE6G
CD93
EVA1A
LINC01163
NREP
ROBO1
MTSS2
LINC00629
ZNF423
−Log10 P
Log2 fold change

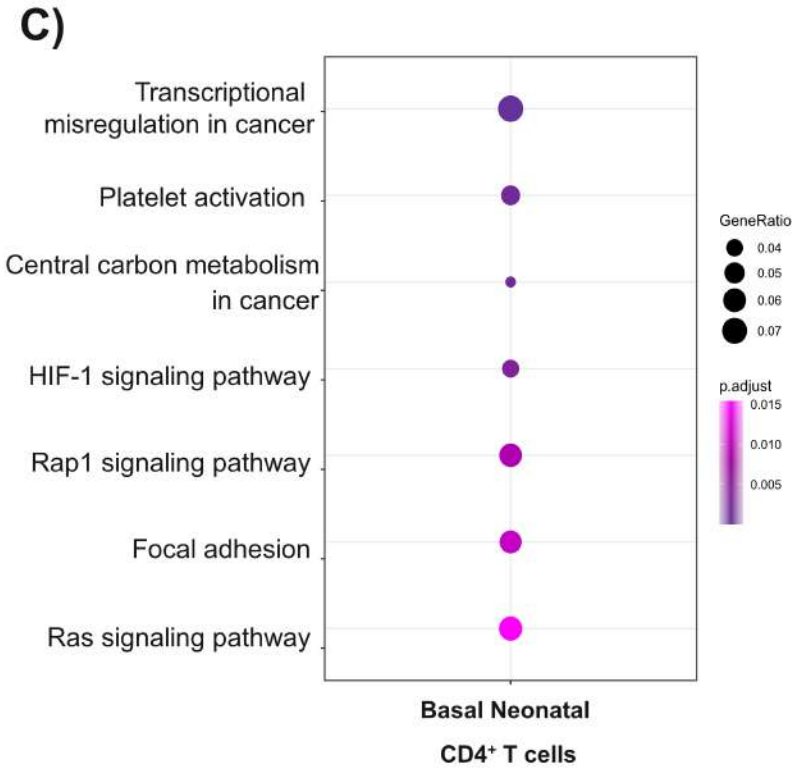
C)
Transcriptional misregulation in cancer
Platelet activation
Central carbon metabolism in cancer
HIF-1 signaling pathway
Rap1 signaling pathway
Focal adhesion
Ras signaling pathway
GeneRatio
p.adjust
Basal Neonatal
CD4+ T cells

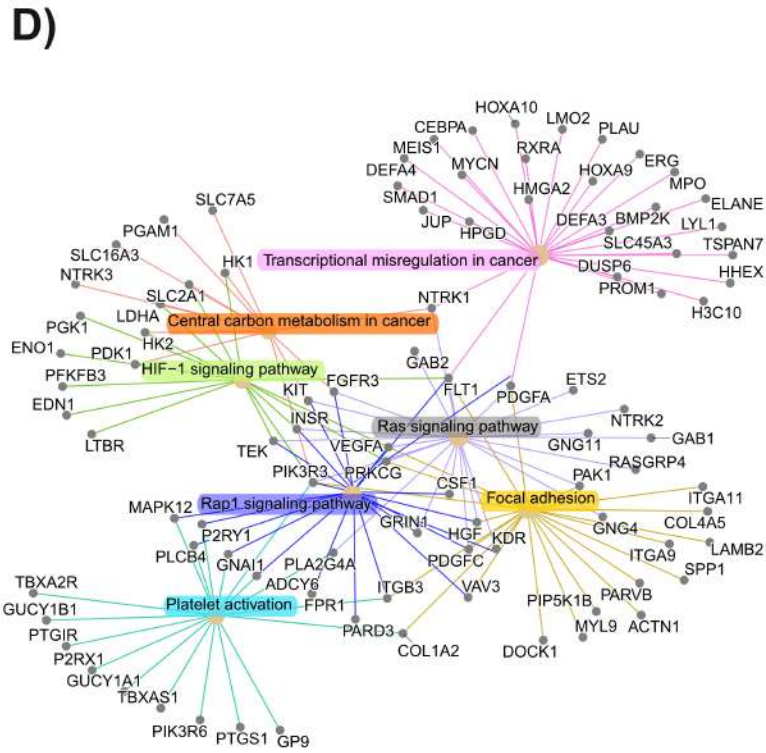
D)
Transcriptional misregulation in cancer
Central carbon metabolism in cancer
HIF−1 signaling pathway
Ras signaling pathway
Rap1 signaling pathway
Focal adhesion
Platelet activation

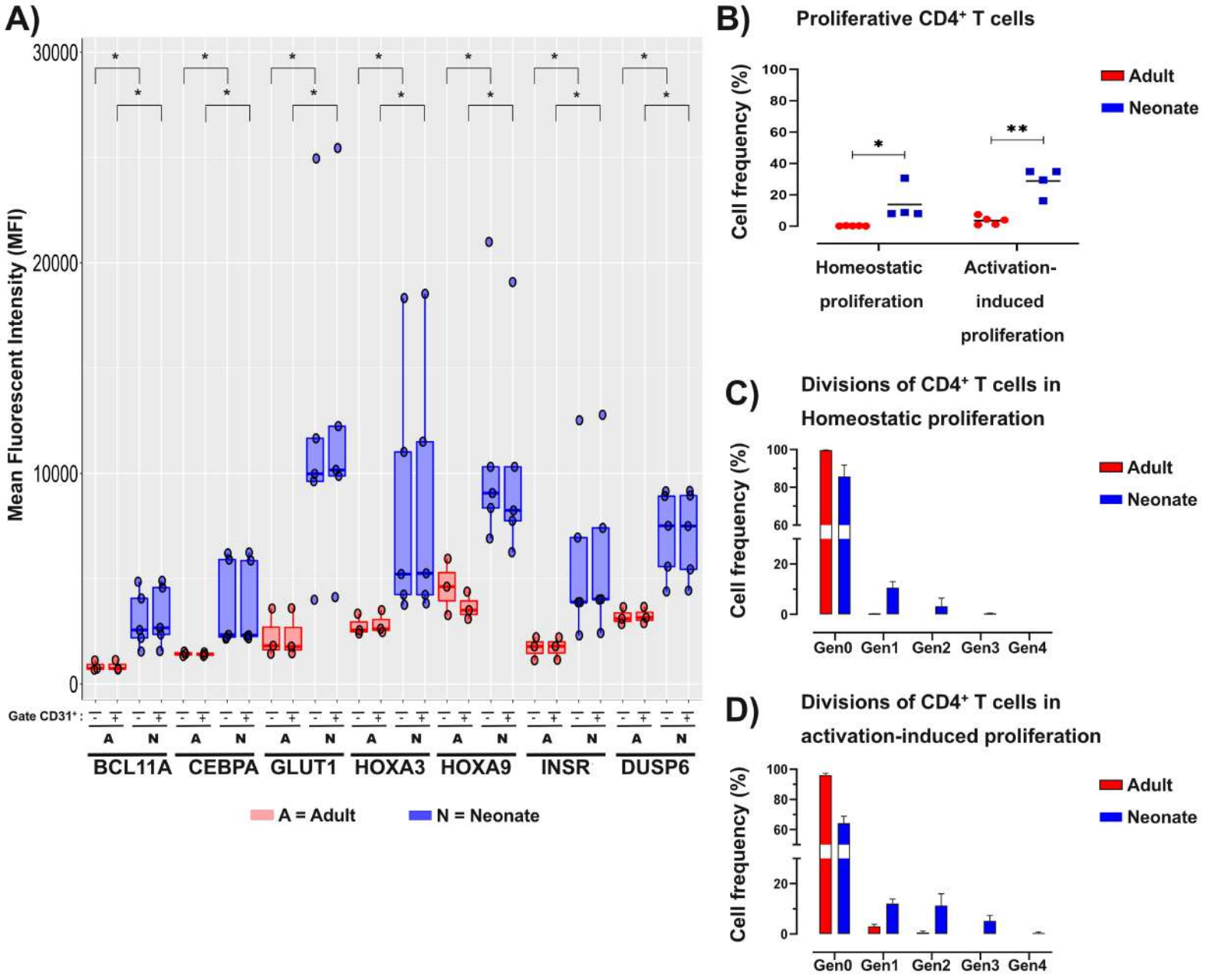
A)
Mean Fluorescent Intensity (MFI)
30000
20000
10000
0
Gate CD31⁺ :
A
N
BCL11A
CEBPA
GLUT1
HOXA3
HOXA9
INSR
DUSP6
A = Adult
N = Neonate
B)
Proliferative CD4⁺ T cells
Cell frequency (%)
Adult
Neonate
Homeostatic proliferation
Activation-induced proliferation
C)
Divisions of CD4⁺ T cells in Homeostatic proliferation
Gen0
Gen1
Gen2
Gen3
Gen4
D)
Divisions of CD4⁺ T cells in activation-induced proliferation

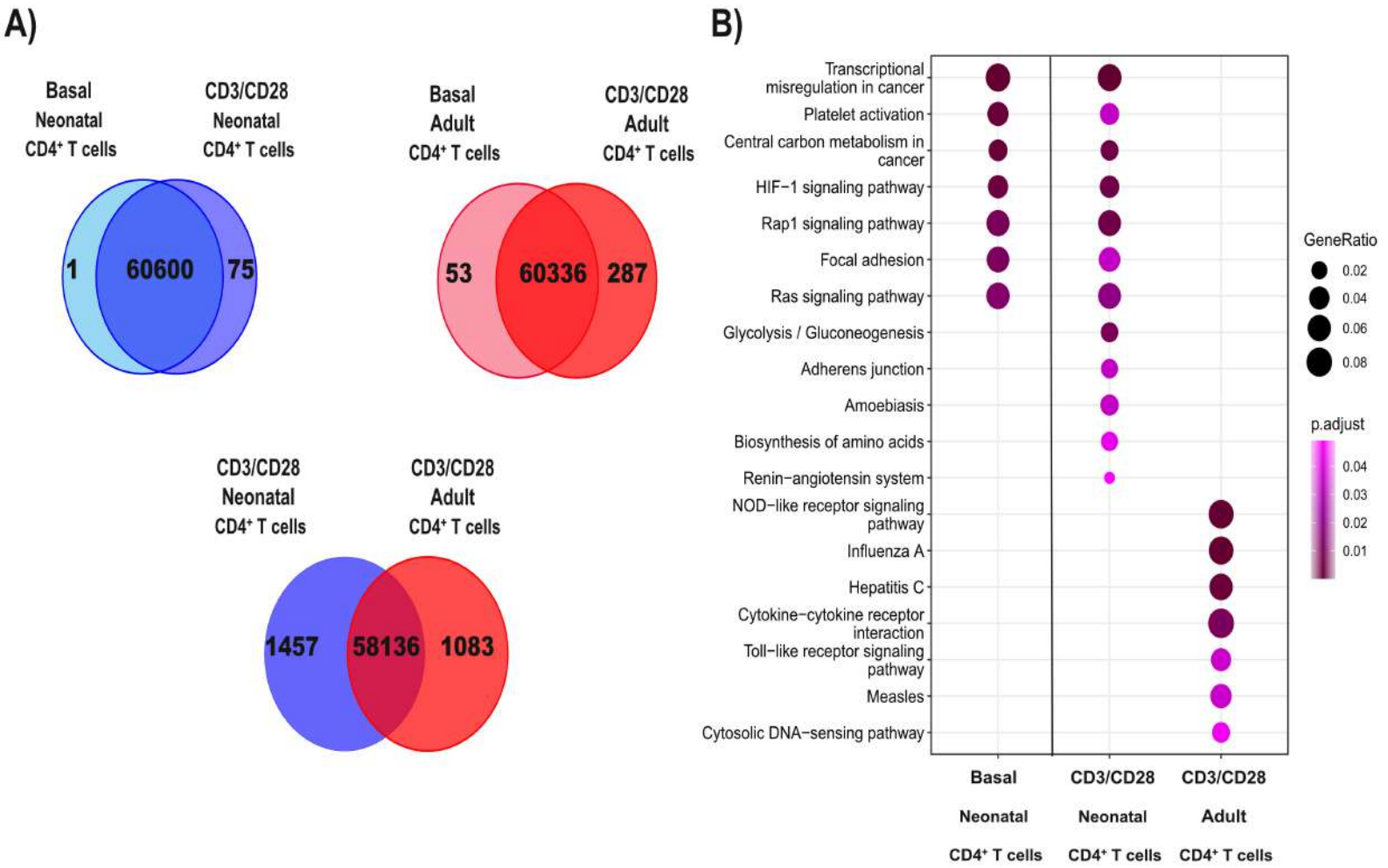
A)
Basal Neonatal CD4+ T cells
CD3/CD28 Neonatal CD4+ T cells
1
60600
75
Basal Adult CD4+ T cells
CD3/CD28 Adult CD4+ T cells
53
60336
287
CD3/CD28 Neonatal CD4+ T cells
CD3/CD28 Adult CD4+ T cells
1457
58136
1083
B)
Transcriptional misregulation in cancer
Platelet activation
Central carbon metabolism in cancer
HIF−1 signaling pathway
Rap1 signaling pathway
Focal adhesion
Ras signaling pathway
Glycolysis / Gluconeogenesis
Adherens junction
Amoebiasis
Biosynthesis of amino acids
Renin−angiotensin system
NOD−like receptor signaling pathway
Influenza A
Hepatitis C
Cytokine−cytokine receptor interaction
Toll−like receptor signaling pathway
Measles
Cytosolic DNA−sensing pathway
Basal Neonatal CD4+ T cells
CD3/CD28 Neonatal CD4+ T cells
CD3/CD28 Adult CD4+ T cells
GeneRatio
0.02
0.04
0.06
0.08
p.adjust
0.04
0.03
0.02
0.01

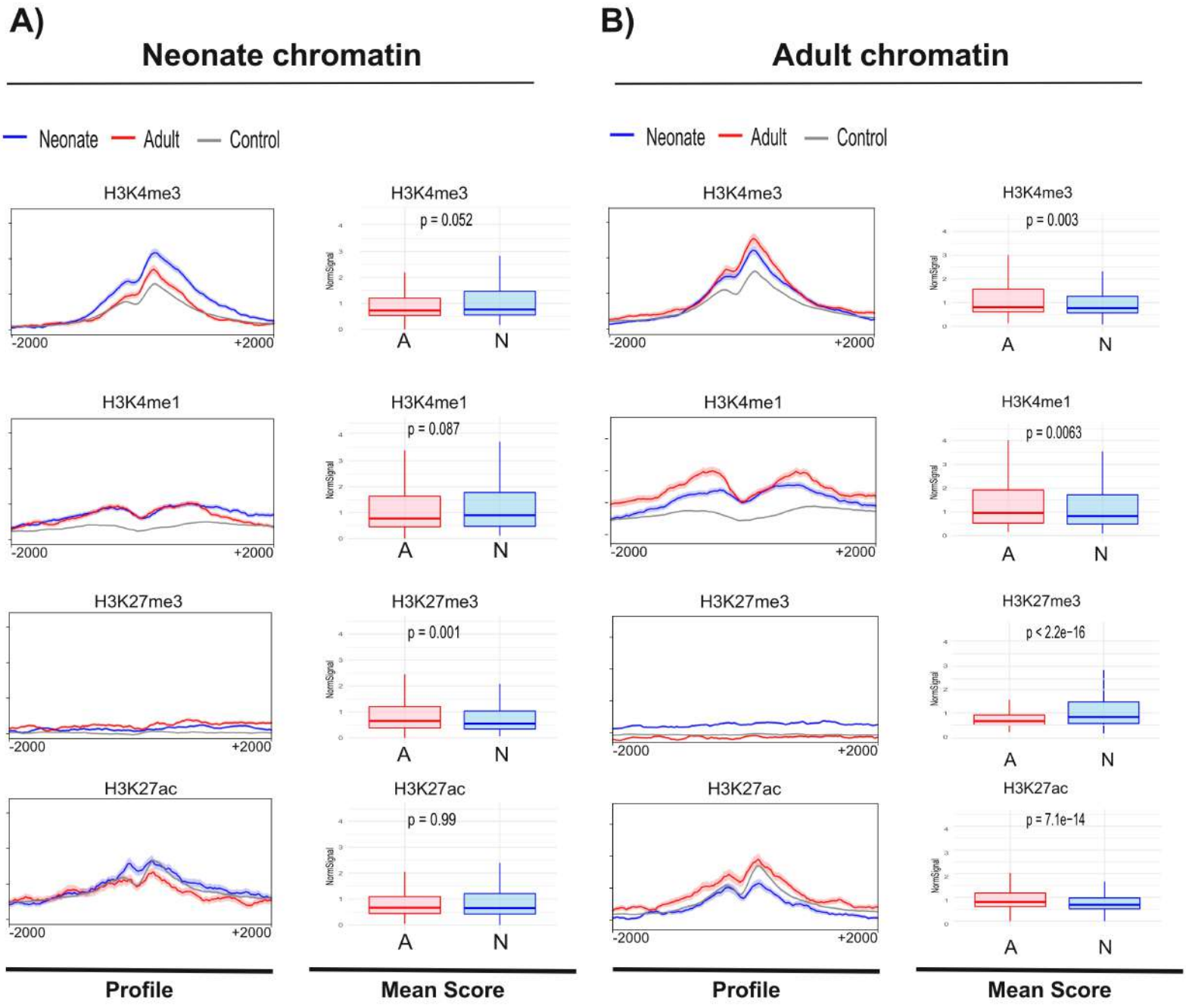
A)
Neonate chromatin
Neonate
Adult
Control
H3K4me3
-2000
+2000
H3K4me1
H3K27me3
H3K27ac
Profile
H3K4me3
p = 0.052
H3K4me1
p = 0.087
H3K27me3
p = 0.001
H3K27ac
p = 0.99
NormSignal
A
N
Mean Score
B)
Adult chromatin
p = 0.003
p = 0.0063
p < 2.2e-16
p = 7.1e-14

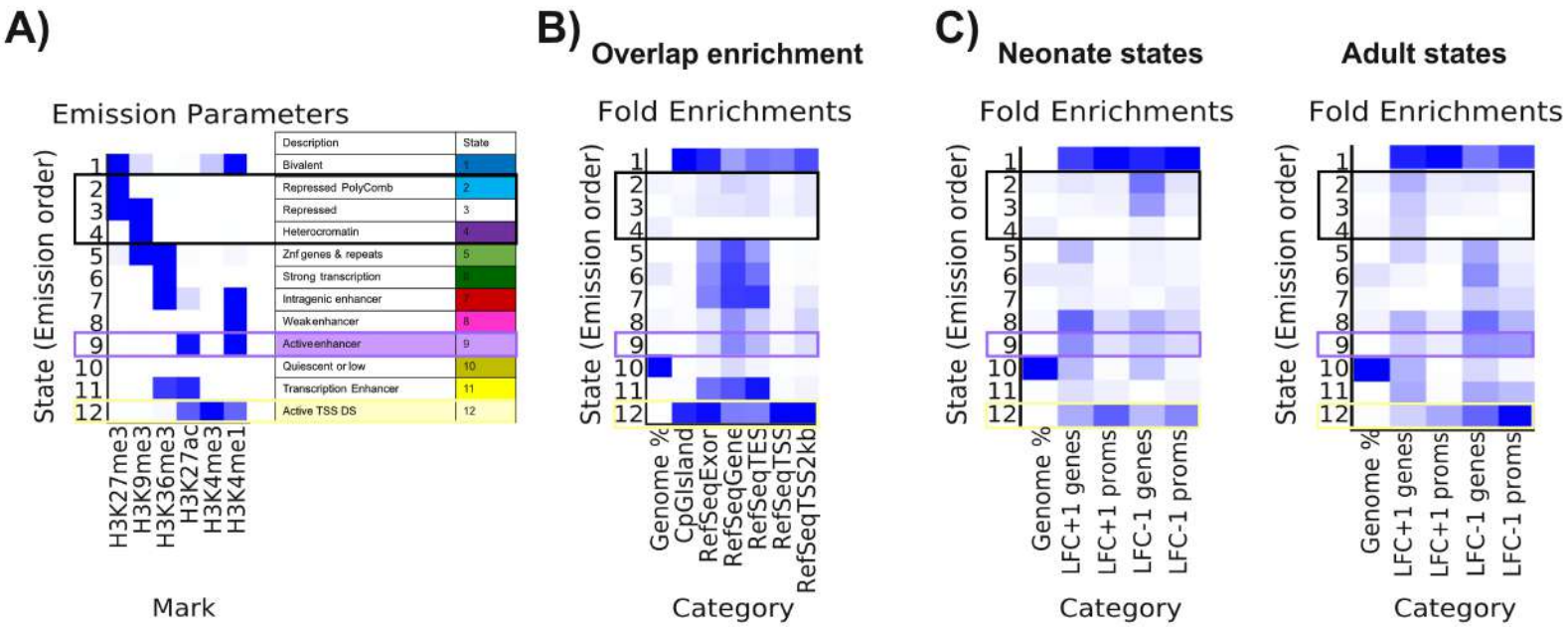
A)
Emission Parameters
State (Emission order)
Description
State
Bivalent
Repressed PolyComb
Repressed
Heterocromatin
Znf genes & repeats
Strong transcription
Intragenic enhancer
Weakenhancer
Activeenhancer
Quiescent or low
Transcription Enhancer
Active TSS DS
H3K27me3
H3K9me3
H3K36me3
H3K27ac
H3K4me3
H3K4me1
Mark
B)
Overlap enrichment
Fold Enrichments
State (Emission order)
Genome %
CpGIsland
RefSeqExon
RefSeqGene
RefSeqTES
RefSeqTSS
RefSeqTSS2kb
Category
C)
Neonate states
Fold Enrichments
State (Emission order)
Genome %
LFC+1 genes
LFC+1 proms
LFC-1 genes
LFC-1 proms
Category
Adult states
Fold Enrichments
State (Emission order)
Genome %
LFC+1 genes
LFC+1 proms
LFC-1 genes
LFC-1 proms
Category

A)

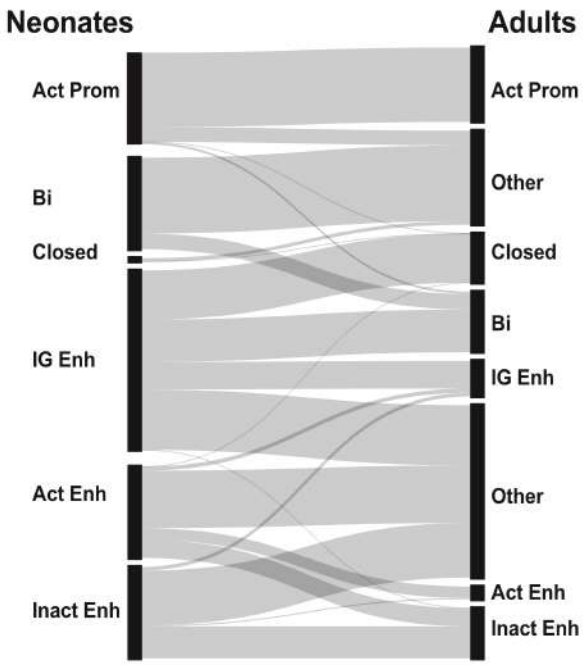

B)

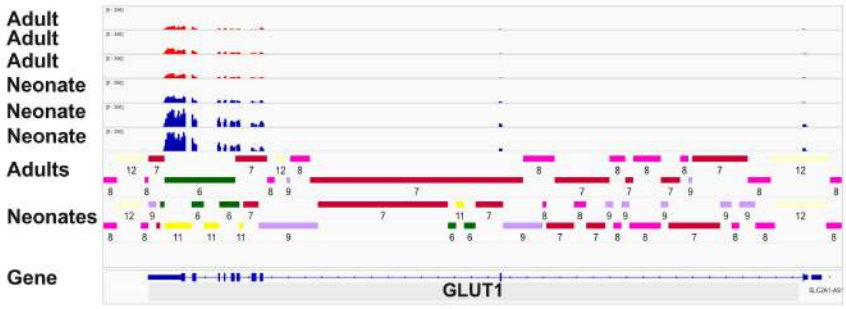

C)

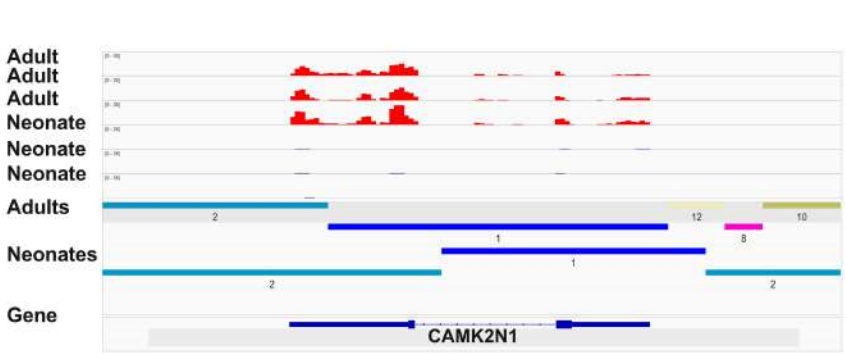

D)

SNPs associations

Regions	trait_id	trait_name	A_count	N_count	A_assoc_count	N_assoc_count	oddsr	p	pcorrect	Enrichment
Prom	ebi-a-GCST002318	Rheumatoid arthritis	13500	9857	89	29	0.4446354	7.60e-05	0.0309117	A
Prom	ebi-a-GCST007800	Asthma (childhood onset)	13500	9857	54	13	0.3288297	9.95e-05	0.0405004	A
Enh	ieu-b-85	Prostate cancer	7651	66133	9	254	3.2737932	4.20e-05	0.0170759	N
Enh	ebi-a-GCST006085	Prostate cancer	7651	66133	9	250	3.2220418	5.72e-05	0.0232951	N

Neonatal CD4⁺ T cells

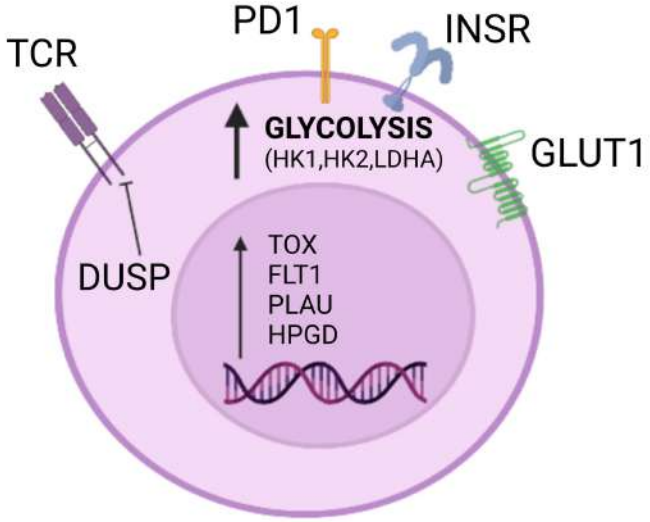

Basal

- ↑ Glycolysis (Genes, receptors, enzymes)
- ↑ Proliferation
- ↓ T cell activation
- ↑ Tolerogenic profile

CD3/ CD28

- ↑↑ Glycolysis (Genes, receptors, enzymes)
- ↑↑ Proliferation
- ↓↓ T cell activation
- ↑↑ Tolerogenic profile

Adult CD4⁺ T cells

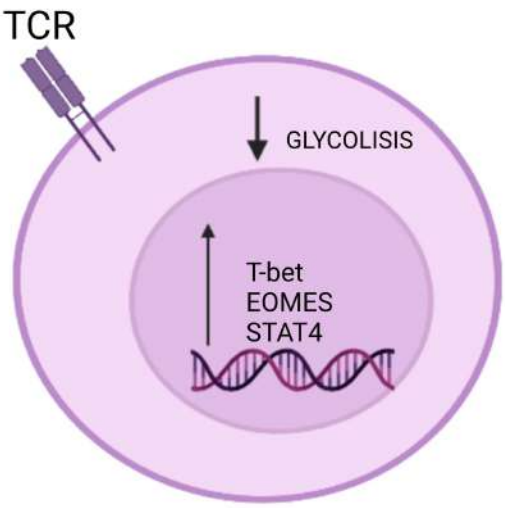

Basal

- ↓ Glycolysis (Genes, receptors, enzymes)
- ↓ Proliferation
- ↑ T cell activation
- ↓ Tolerogenic profile

CD3/ CD28

- ↓↓ Glycolysis (Genes, receptors, enzymes)
- ↑ Proliferation
- ↑↑ T cell activation
- ↓↓ Tolerogenic profile